UNIVERSITY OF BIRMINGHAM
University of Birmingham Research at Birmingham

To see, or not to see? Rifted margin extension

McDermott, Kenneth; Reston, Timothy

DOI:
10.1130/G36982.1

License:
None: All rights reserved

Document Version
Peer reviewed version

Citation for published version (Harvard):
McDermott, K & Reston, T 2015, 'To see, or not to see? Rifted margin extension', *Geology*, vol. 43, no. 11, pp. 967-970. https://doi.org/10.1130/G36982.1

Link to publication on Research at Birmingham portal

Publisher Rights Statement:
Checked October 2015

General rights
Unless a licence is specified above, all rights (including copyright and moral rights) in this document are retained by the authors and/or the copyright holders. The express permission of the copyright holder must be obtained for any use of this material other than for purposes permitted by law.

•Users may freely distribute the URL that is used to identify this publication.
•Users may download and/or print one copy of the publication from the University of Birmingham research portal for the purpose of private study or non-commercial research.
•User may use extracts from the document in line with the concept of 'fair dealing' under the Copyright, Designs and Patents Act 1988 (?)
•Users may not further distribute the material nor use it for the purposes of commercial gain.

Where a licence is displayed above, please note the terms and conditions of the licence govern your use of this document.

When citing, please reference the published version.

Take down policy
While the University of Birmingham exercises care and attention in making items available there are rare occasions when an item has been uploaded in error or has been deemed to be commercially or otherwise sensitive.

If you believe that this is the case for this document, please contact UBIRA@lists.bham.ac.uk providing details and we will remove access to the work immediately and investigate.

Download date: 05. May. 2023

Publisher: GSA
Journal: GEOL: Geology
DOI:10.1130/G36982.1

To see, or not to see? Rifted margin extension

Ken McDermott* and Tim Reston
School of Geography, Earth and Environmental Sciences, University of Birmingham, Birmingham B15 2TT, UK
*Current address: ION, 1st Floor, Integra House, Vicarage Road, Egham, Surrey TW20 9JZ, UK.

ABSTRACT

A characteristic of rifted margins is the extension discrepancy: i.e., the amount of extension estimated from fault geometries on seismic images is far too little to explain the observed crustal thinning and subsidence. Either the crust has been thinned in some other way or the amount of extension has been severely underestimated. To investigate the latter, we create a model structural section across a rifted margin by focusing extension in the center of a rift, producing successive phases of crosscutting faults. From one side of this section, a synthetic seismic image is generated and interpreted as if it were a real profile. Just as for real margins, apparent listric faults and eroded fault block crests are seen, but these are not present in the model and instead represent intersecting fault surfaces, and are thus diagnostic of polyphase faulting. Just as for real margins, the amount of extension measured from the seismic is only a fraction of the true extension. Just as for real margins, this extension discrepancy increases markedly oceanward. Demonstrably for the synthetic margin, and by implication for real margins, the extension discrepancy is the failure of the seismic method to image unambiguously the polyphase faulting required to accommodate increasing extension, combined with a general lack of awareness of the features, outlined here, diagnostic of such faulting.

INTRODUCTION

Our limited understanding of the breakup of the continents to form the ocean basins is based on sparse well data and seismic images of rifted margins, which typically appear as an apparently simple series of tilted fault blocks (e.g., Ranero and Pérez-Gussinyé, 2010; Doré and Lundin, 2015) beneath the postrift cover. However, too little extension can be measured from the geometries of the faults to explain the observed thinning and subsidence (Davis and Kusznir, 2004). Addressing this extension discrepancy has become a benchmark test for models of rifting and breakup (Doré and Lundin, 2015). There are two end-member solutions (Reston, 2007): either the amount of extension has been severely underestimated, or, if the observed faulting represents all the upper crustal extension, the deeper crust has been further thinned by depth-dependent thinning (Kusznir and Karner, 2007; Huismans and Beaumont, 2008). In this paper we generate a synthetic seismic profile (Fig. 1) from a model geological section produced by the relatively simple processes likely to occur as rifting progresses toward breakup. The results show how an extension discrepancy, similar to that observed at real margins, is a natural consequence of those processes and of the limitations of the seismic method, removing the need for most of the complex models proposed.

SYNTHETIC SEISMIC IMAGE OF A RIFTED MARGIN

When studying a real seismic section, the interpreter does not know the geometries that produced it. To replicate such interpretation as much as possible, we start

by showing a synthetic seismic section (Fig. 1A), which can thus be examined and interpreted with no prior knowledge of the two-dimensional (2-D) geological model (described later) used to generate it. The synthetic section is generated using image rays (Hubral, 1977); a small amount of noise has been added and the synthetic data filtered to more closely mimic real data across a rifted margin, but the image remains as good as the best possible 3-D time migration of real data and superior to that likely to be encountered if a thick or complex postrift succession is present.

Interpretation of the synthetic section (Fig. 1B) identifies a simple series of fault blocks bounded by oceanward-dipping listric faults; one fault exhibits a ramp-flat geometry above which the hanging wall is folded. Some blocks have planed-off crests, perhaps indicative of mass wasting or subaerial erosion during rifting, and all are overlain by synrift sedimentary wedges thickening toward the fault. To the right, the seafloor and the basement blocks deepen, and the listric faults merge downward into a seaward-dipping band of reflections resembling a detachment system. Summing the heaves at the top of the basement gives an average stretching factor of 1.46 across the entire section, but there is little increase in the measured extension from left to right; successive groups of 3–4 fault blocks all have mean seismically derived stretching factors (β_{seis}) of just <1.5, similar to those measured at rifted margins, where they are commonly taken (e.g., Davis and Kusznir, 2004) to represent the amount of upper crustal extension.

Although the details might differ slightly, we are confident that most interpreters would come to similar conclusions. However, the model (Fig. 2) used to generate the synthetic image is quite different. In an initially broad rift, extension progressively focuses in the rift axis where extension is greatest (Fig. 2A), as in the North Sea (Cowie et al., 2005). The modeled extension is by slip on faults and differential fault block rotation, accommodated by minor internal deformation; the geometries resemble those predicted by flexural cantilever modeling (Kusznir et al., 1995) with moderate elastic thicknesses (~5 km). As extension focuses, the outer faults are abandoned (Cowie et al., 2005) and the inner faults rotated to lower angle until, at a local stretching factor of ~1.6, it becomes easier for new faults to form at ~60°–70° to horizontal (Jackson and White, 1989) than for slip to continue on the old faults, which become locked (Fig. 2A). However, as extension continues to focus in the rift axis (Fig. 2B) the new faults also rotate to low angles, become locked, and are cut by a third generation, producing complex geometries (Proffett, 1977; Jackson and White, 1989) that would be less distinct with lower elastic thicknesses or more internal block deformation. The final stage (Fig. 2C) is used, after assigning appropriate velocities and densities (e.g., Lau et al., 2006; Fig. 2C), to generate the synthetic image; intrabasement faults are modeled as 15-m-thick layers with 10% seismic anisotropy, similar to the properties of real faults (Jones and Nur, 1984).

Comparing Figure 1B with the input model (Fig. 2C) shows that many details of the interpretation are incorrect. Downward-increasing seismic velocity coupled with the back-tilting of the fault blocks makes even planar faults appear somewhat listric, but the most listric are actually combinations of different generations of faults, as are the apparent ramp-flat geometry and the overlying “hanging-wall fold” (Fig. 1B). There is no detachment system; segments of older and younger faults appear to merge into a system that was never active at a low angle or simultaneously. The apparent erosion of the tops

Publisher: GSA
Journal: GEOL: Geology
DOI:10.1130/G36982.1
of the fault blocks (Fig. 1B) is also the intersection of two fault generations; in this case, the downward truncation of an early fault (rotated to low angle) by a steeper later fault.

Many of the features identified in Figure 1B are not present in Figure 2C, whereas most of the key extensional structures are so distorted on the time section (Fig. 2D) that they are unlikely to be recognized. Measuring all the faults gives a true stretching factor (β_{true}) that matches crustal thinning and increases to the right (Fig. 2C) from 1.5 (1 phase of faulting) to 2.9 (2 phases) to 3.8 (3 phases), but at any point on the synthetic section only the latest phase of faulting is readily interpretable, giving a seismic stretching factor (β_{seis}) in each domain of just <1.5 (Fig. 1B). The discrepancy between β_{true} and β_{seis} (and the corresponding thinning factors) increases oceanward, just like the extension discrepancy observed at rifted margins (Fig. 3; Kusznir and Karner, 2007). As the extension discrepancy in this synthetic example is demonstrably the result of the failure of the seismic method to identify all the faulting, the implication is that the very similar discrepancy observed at real margins (Fig. 3) may have the same cause.

RECOGNIZING POLYPHASE FAULTING

Davis and Kusznir (2004) and Ranero and Pérez-Gussinyé (2010), among others, claimed that seismic data across margins show no evidence for crosscutting faulting, but did not specify how they might have recognized it. Our modeling identifies several possible diagnostic features and indicates why they are so easily overlooked.

Most real intrabasement faults juxtapose similar lithologies and have only moderate internal anisotropy (Jones and Nur, 1984), and so do not give rise to strong reflections. Similarly, the synthetic reflections from such faults are far weaker than those from top basement, and are distorted by the variable velocity of the overlying fault blocks, producing a complex pattern of short, weak reflection segments that is liable to be misinterpreted. For example, an old intrabasement fault segment dipping in the same direction as a younger fault may be misinterpreted as part of a detachment system (Fig. 1B) or as a listric fault (IV in Fig. 4A).

Fault-fault intersections may be easier to identify if they occur at the top of the basement rather than within the basement. However, a gently dipping old fault intersecting downward with a younger, steeper one can be misinterpreted on a time migration as an eroded or mass-wasted fault block crest (I in Fig. 4A) or simply as a single slightly convex-upward fault (II in Fig. 4A; Reston and McDermott, 2014). Polyphase faulting is more likely to be recognized if the older top-basement fault is in the hanging wall of a younger steeper fault dipping in the same direction (V in Fig. 4A; Reston and McDermott, 2014).

Unless the top of the basement had been previously rotated from horizontal, normal faults should form at a hanging-wall angle of 60°–70° to it. This angle should be reduced by internal block deformation, but where it increases to 80° or more (III in Fig. 4A), it implies that the basement was pre-rotated, for example by earlier faulting. However, such diagnostic angular relationships are not accurately represented on time sections. On such sections, identification of multiple and overlapping synrift wedges might offer the best chance of regularly identifying polyphase faulting, but many margins are sediment starved and exhibit only thin, condensed synrift sequences, easily mistaken for prerift sequences (Reston and McDermott, 2014).

These features can only be recognized on good seismic images of rifted margins if the interpreter is actively looking for them. Depth imaging helps, but only reveals the true, undistorted geometries if constructed using the correct velocity model, and intrabasement reflections remain weak and intermittent. The issues are highlighted by comparing depth and time sections (Deemer et al., 2009; Lau et al., 2006) across the Newfoundland Basin margin (Figs. 4B and 4C), where there is an extension discrepancy similar to both the synthetic margin and to other real margins (Fig. 3). Early faults might be interpreted on the depth section from the geometry of the top of the basement, but this could easily be taken as evidence of mass wasting or erosion (II in Figs. 4B and 4C) or as a fold (Lau et al., 2006). Weak, gently dipping intrabasement reflections may be from early faults rather than a detachment system (IV in Figs. 4B and 4C). A previous phase of faulting can be inferred from the ~80° angle between late faults and the top of the basement (III in Fig. 4B), but the angles are not apparent on the time section (Fig. 4C). In summary, crosscutting faults that might be identified through careful interpretation of a depth section are far less recognizable in time.

DISCUSSION AND CONCLUSIONS

We have shown that polyphase crosscutting faulting should be expected at rifted margins, but can be recognized only if actively and carefully sought; failure to recognize it provides a simple explanation for the extension discrepancy.

Other explanations have been advanced, with very different implications for the process of rifting to breakup. Ranero and Pérez-Gussinyé (2010, p. 294) suggested that, even if all the faulting was “unambiguously visible,” asymmetric migration of the locus of extension into the rift flank through sequential faulting could explain the extension discrepancy. However, their model only led to an overall discrepancy across the margin because, although the rifting migrated across crust that had already been extended, only the slip on the later faults was compared to the total thinning (Reston and McDermott, 2014); as proposed here it was unidentified early extension that produced an extension discrepancy. The fractal distribution of fault sizes means that perhaps 30% of the extension is taken up along faults too small to be resolved by the seismic method (Walsh and Watterson, 1992), explaining the minor discrepancy noted in rift basins (Marrett and Allmendinger, 1992) and near the shelf, but not the magnitude of the discrepancy observed at the deep margin (Davis and Kusznir, 2004; Reston and McDermott, 2014). This contrast led Kusznir and Karner (2007) to propose that rifting to break up a continent is fundamentally different from rifting to form a basin, with depth-dependent thinning (DDT) occurring near breakup and after fault block rotation and erosion (Davis and Kusznir, 2004). However, any erosion may indicate the presence of polyphase faulting rather than subaerial exposure; those geodynamic models that predict a degree of crustal DDT (Huismans and Beaumont, 2008) do so during, not after, rifting. Furthermore, to maintain cross-sectional areas, the excess thinning of the middle and lower crust that defines DDT must be balanced elsewhere by excess thinning of the upper crust and/or by thickening of the middle and lower crust, neither of which has to our knowledge been reported (e.g., Fig. 3); wide-angle data nowhere show DDT on the scale required (Reston, 2007).

We conclude that crosscutting polyphase faulting, combined with some degree of distributed deformation, both of which are to be expected but difficult to recognize at

rifted margins, provides the best explanation for the extension discrepancy at rifted margins and that more complex geodynamic models are not required.

ACKNOWLEDGMENTS

We thank Ian Fairchild and reviewers Tony Dor**é**, Chris Jackson, and Alan Roberts for insightful comments. Modelling used the NORSAR software (www.norsar.no/seismod/home/) and processing used Globe Claritas (www.globeclaritas.com). Funding by the Natural Environment Research Council (grant NE/E015883/1), the University of Birmingham, and the Irish Petroleum Infrastructure Programme/Expanded Offshore Support Group (PIP/EOSG) is gratefully acknowledged.

REFERENCES CITED

Cowie, P.A., Underhill, J.R., Behn, M.D., Lin, J., and Gill, C.E., 2005, Spatio-temporal evolution of strain accumulation derived from multi-scale observations of Late Jurassic rifting in the northern North Sea: A critical test of models for lithospheric extension: Earth and Planetary Science Letters, v. 234, p. 401–419, doi:10.1016/j.epsl.2005.01.039.

Davis, M., and Kusznir, N.J., 2004, Depth-dependent lithospheric stretching at rifted continental margins, *in* Karner, G.D., ed., Proceedings of the National Science Foundation Rifted Margins Theoretical Institute: New York, Columbia University Press, p. 92–136.

Deemer, S., Hall, J., Solvason, K., Lau, K.W.H., Louden, K.E., Srivastava, S., and Sibuet, J.C., 2009, Structure and development of the southeast Newfoundland continental passive margin: Derived from SCREECH Transect 3: Geophysical Journal International, v. 178, p. 1004–1020, doi:10.1111/j.1365–246X.2009.04162.x.

Doré, T., and Lundin, E., 2015, Hyperextended continental margins: Knowns and unknowns: Geology, v. 43, p. 95–96, doi:10.1130/focus012015.1.

Hubral, P., 1977, Time-migration—Some ray-theoretical aspects: Geophysical Prospecting, v. 25, p. 738–745, doi:10.1111/j.1365-2478.1977.tb01200.x.

Huismans, R.S., and Beaumont, C., 2008, Complex rifted continental margins explained by dynamical models of depth-dependent lithospheric extension: Geology, v. 36, p. 163–166, doi:10.1130/G24231A.1.

Jackson, J.A., and White, N.J., 1989, Normal faulting in the upper continental crust: Observation from regions of active extension: Journal of Structural Geology, v. 11, p. 15–36, doi:10.1016/0191-8141(89)90033-3.

Jones, T., and Nur, A., 1984, The nature of seismic reflections from deep crustal fault zones: Journal of Geophysical Research, v. 89, p. 3153–3171, doi:10.1029/JB089iB05p03153.

Kusznir, N., and Karner, G., 2007, Continental lithospheric thinning and breakup in response to upwelling divergent mantle flow: Application to the Woodlark, Newfoundland and Iberia margins, *in* Karner, G.D., et al., eds., Imaging, mapping and modelling continental lithosphere extension and breakup: Geological Society of London Special Publication 282, p. 389–419, doi:10.1144/SP282.16.

Kusznir, N.J., Roberts, A.M., and Morley, C.K., 1995, Forward and reverse modelling of rift basin formation, *in* Lambiase, J.J., ed., Hydrocarbon habitat in rift basins:

Geological Society of London Special Publication 80, p. 33–56, doi:10.1144/GSL.SP.1995.080.01.02.

Lau, K.W.H., Louden, K.E., Deemer, S., Hall, J., Hopper, J.R., Tucholke, B.E., Holbrook, W.S., and Larsen, H.C., 2006, Crustal structure across the Grand Banks–Newfoundland Basin continental margin–II. Results from a seismic reflection profile: Geophysical Journal International, v. 167, p. 157–170, doi:10.1111/j.1365-246X.2006.02989.x.

Marrett, R., and Allmendinger, R., 1992, Amount of extension on "small" faults: An example from the Viking graben: Geology, v. 20, p. 47–50, doi:10.1130/0091-7613(1992)020<0047:AOEOSF>2.3.CO;2.

Proffett, J.M., 1977, Cenozoic geology of the Yerington district, Nevada, and implications for the nature of Basin and Range faulting: Geological Society of America Bulletin, v. 88, p. 247–266, doi:10.1130/0016-7606(1977)88<247:CGOTYD>2.0.CO;2.

Ranero, C.R., and Pérez-Gussinyé, M., 2010, Sequential faulting explains the asymmetry and extension discrepancy of conjugate margins: Nature, v. 468, p. 294–299, doi:10.1038/nature09520.

Reston, T.J., 2007, The extension discrepancy at North Atlantic non-volcanic rifted margins: Depth-dependent stretching or unrecognized faulting?: Geology, v. 35, p. 367–370, doi:10.1130/G23213A.1.

Reston, T.J., and McDermott, K., 2014, An assessment of the cause of the "Extension Discrepancy" with reference to the west Galicia margin: Basin Research, v. 26, p. 135–153, doi:10.1111/bre.12042.

Walsh, J., and Watterson, J., 1992, Populations of faults and fault displacements and their effects on estimates of fault-related regional extension: Journal of Structural Geology, v. 14, p. 701–712, doi:10.1016/0191-8141(92)90127-I.

Publisher: GSA
Journal: GEOL: Geology
DOI:10.1130/G36982.1

FIGURES

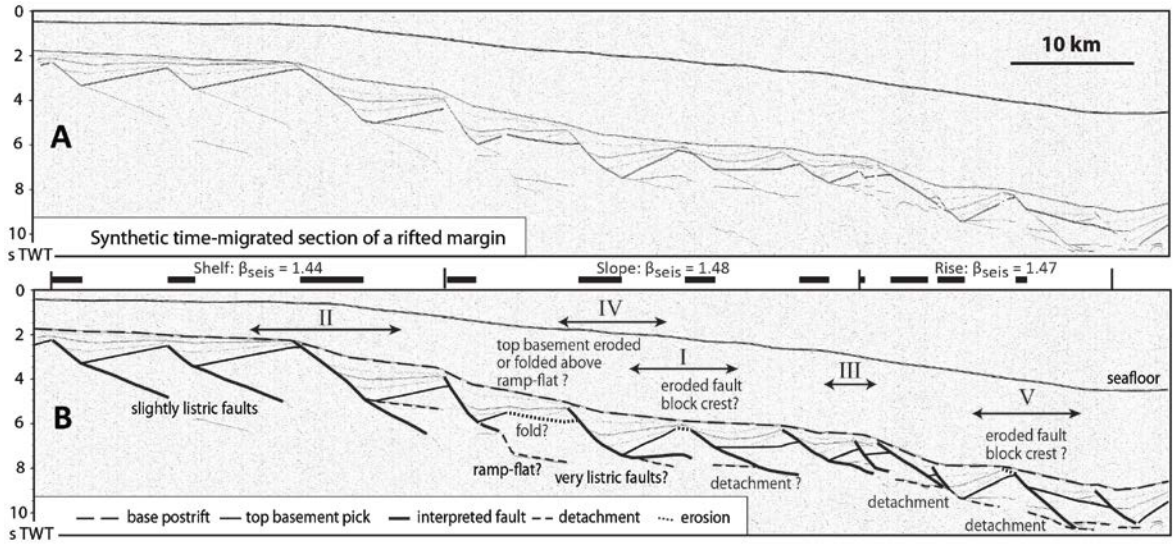

Figure 1. A: Synthetic seismic section across model rifted margin. TWT—two-way traveltime. B: Interpretation showing well-defined fault blocks and synrift wedges bounded by listric faults, which to the right merge into a well-defined detachment system. The crests of several fault blocks appear eroded, suggesting they were near sea level toward the end of rifting. Summing the heaves provides an estimate of the total extension. Most of these interpretations are incorrect: the faults are not so listric, there is no detachment system, the crests of the fault blocks have not been eroded and were not at sea level during late rifting, and the observed fault heaves only show a fraction of the total extension. Roman numerals refer to features shown in Figure 4. β_{seis}—seismically derived stretching factor.

Publisher: GSA
Journal: GEOL: Geology
DOI:10.1130/G36982.1

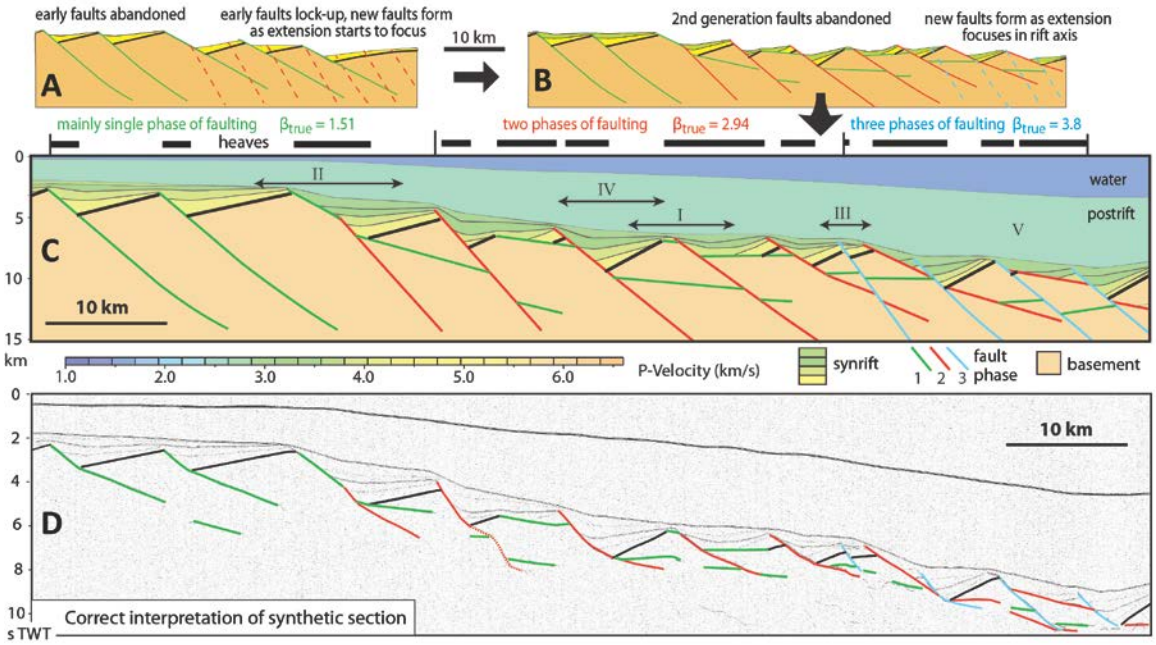

Figure 2. Kinematic model focusing extension in the rift axis via three phases of crosscutting faults, producing complex geometries. A: One side of rift during early extension. Near the rift axis, faults rotate to <40° and become locked; new faults cut across them. β_{true}—true stretching factor. B: Extension continues along new faults until these in turn become locked and a third generation of crosscutting faults develops near the axis. C: The final stage, after deposition of a thick postrift sequence (shown unreflective), used to produce the synthetic seismic section (Fig. 1A). Roman numerals refer to features shown in Figure 4. D: The correct interpretation of the synthetic seismic section. Simple structures have been distorted by the overlying velocity structure, the faults are not so listric, there is no detachment system, and the crests of late fault blocks have been shaped by earlier faulting rather than eroded. The total amount of extension is approximately twice that interpreted in Figure 1, with considerably more extension further oceanward. TWT—two-way traveltime.

Publisher: GSA
Journal: GEOL: Geology
DOI:10.1130/G36982.1

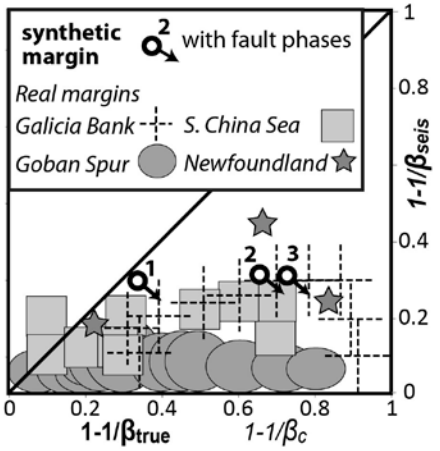

Figure 3. Cross-plot of thinning factors. Circles represent average thinning factors from interpreted fault heaves in Figure 1B ($1 – 1/\beta_{seis}$) and from true geometry of faults shown in Figure 2C ($1 – 1/\beta_{true}$) for the parts of the model margin with one (left), two (middle), and three (right) phases of faulting. Where there is more than one phase of faulting, the interpretation severely underestimates the amount of thinning. Arrows show increase in extension discrepancy if ~30% distributed deformation was included. Plotted for comparison are thinning factors from crustal thinning ($1 – 1/\beta_c$) and seismic imaging ($1 – 1/\beta_{seis}$) across the Galicia, Goban Spur (northeastern Atlantic Ocean), and the South (S.) China Sea margins (all from Davis and Kusznir, 2004) and from the South Newfoundland Basin (Fig. 4). All plot overwhelmingly in the bottom right quadrant, indicating substantially more thinning than fault-measured extension.

Publisher: GSA
Journal: GEOL: Geology
DOI:10.1130/G36982.1

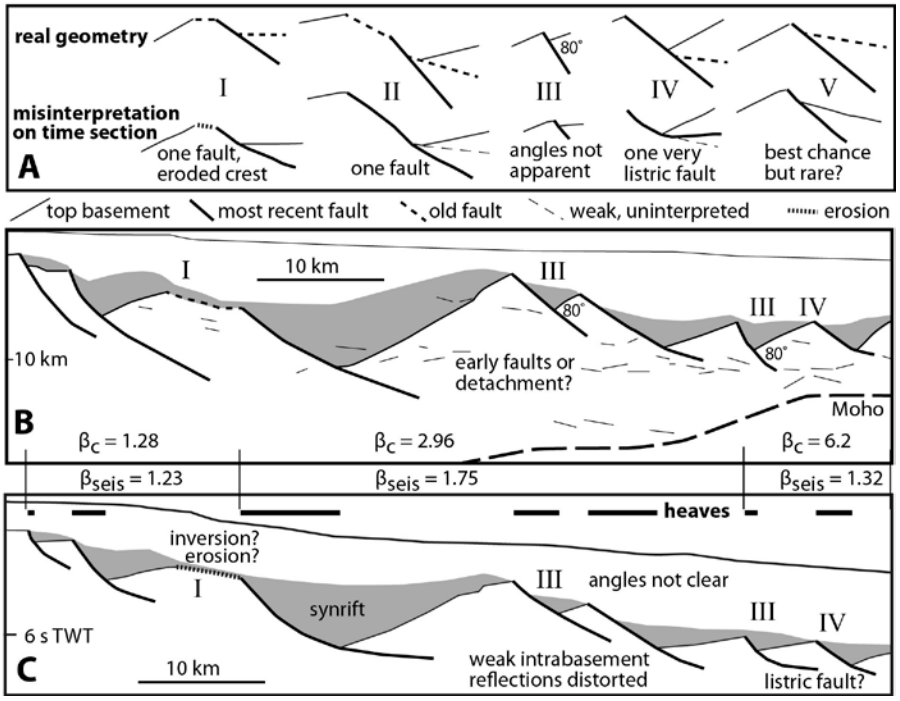

Figure 4. Features potentially diagnostic of crosscutting faulting. A: Real geometry (from Fig. 2C) and likely misinterpretation on time sections (from Fig. 1B). I, II—intersection of two faults at the level of the top of the basement, misinterpreted as an eroded fault block (I) or a single convex-upward fault (II); III—intersection of late fault with top basement at angles >70°, not measurable on a time section; IV—intersection of two faults within basement misinterpreted as a listric fault; V—old fault in hanging wall of a young fault, misinterpreted as top of the basement. B: Identification of three of these diagnostic features (I, III, IV) on depth section of SCREECH3 (Studies of Continental Rifting and Extension on the Eastern Canadian Shelf) across the Newfoundland margin (geometries of Deemer et al., 2009, reinterpreted). C: Difficulty in identification from equivalent geometries on time section. Stretching factors from summing fault heaves (β_{seis}, seismically derived) and from crustal thinning (β_c) within the three domains defined by vertical bars are plotted in Figure 3. TWT—two-way traveltime.